Journal of Fluorescence (2019) 29:899–909
https://doi.org/10.1007/s10895-019-02402-3

ORIGINAL ARTICLE

# An Experimental and Theoretical Test of Dielectric Friction Models Using Rotational Diffusion of 7-Diethylamino-2-H-1-Benzopyran-2-One in Non-associative Solvents

Anil Kumar[1] · C. G. Renuka[2] · Y. F. Nadaf[3]

Received: 1 March 2019 / Accepted: 10 June 2019 / Published online: 4 July 2019


**Abstract**
The rotational re-orientations times of the 7-DHB dye molecule have been examined in non-associative solvents (DMSO and Octanenitrile) by varying the temperature, by employing the Steady-State Fluorescence Depolarisation and Time-Correlated Single Photon Counting (TCSPC) techniques. Rotational re-orientations time values in DMSO are found larger by a factor of 1.136 than octanenitrile, which indicates that 7-DHB laser dye is experiencing higher friction in DMSO than octanenitrile. To determine mechanical friction Stokes Einstein's Debye theory (SED) -with a stick, slip boundary conditions parameters are used and found an interesting super slip trend. Point dipole models as Nee-Zwanzig (NZ) and van der Zwan-Hynes (ZH) fail to explain experimental dielectric friction observed trends. Alavi-Waldeck model successfully explains the observed dielectric friction trend in non-associative solvents.

**Keywords** Diffusion · Molecular correlation · Non-associative solvents · Dielectric theories · Charge distribution

## Introduction

A molecule rotating in solution experience frictions because of its continuous interactions with its surrounding. The molecular motions may be restricted or free depending on the physical and chemical properties of the surrounding medium. In a free solvent, medium rotational and translational diffusion molecular motions occur for any solute. Study of the rotational and translational diffusion molecules are of key importance because it leads to an understanding of the dynamic interaction with surrounding molecules such as solvent-solute interactions. Solute molecular rotations will function as a sensitive probe of molecular structure and molecular dynamics, far more results than translation motion. Molecular correlation times provide useful information on the results of chemical interest like aggregations, solvation's, photochemical process, isomerization, hydrogen bonding and many other [1]. A good understanding of the molecular correlation functions and correlation times tell us regarding what's occurring in the immediate neighborhood of the rotating probe molecules. The studies of rotational reorientation dynamics are broadly classified into two categories, [2] Firstly, Polar probes embedded in charged polar solvents to know how the electrostatic long-range interaction influences the rotational dynamics of the solute molecule. Secondly, non-polar probes embedded in non-polar or polar solvents to understand the influence solute to solvent size ratio and solute shape.

The diffusion motion of large solute molecules is generally described by Brownian motion theories [3]. The hydrodynamic basis for determining the rotational friction experienced by a sphere rotating in a solvent is given by Einstein [4]. The theoretical descriptions of the molecular rotational motion of any probe in the liquid are described by Stokes, Einstein's, Debye, Perrin equations, the rotational reorientation time ($\tau_r$) of the solute is related to the solvent viscosity parameter ($\eta$). Most often the molecules are not spherical consequently, the

✉ Y. F. Nadaf
dryfnadaf@gmail.com

[1] P.G. Department of Physics, Sri Siddeshwara Government First Grade College, Naragund 582207, India

[2] Department of Physics, Jnanabharathi campus, Bangalore University, Bengaluru 560056, India

[3] Department of Physics and Research Center, Maharani Science College for Women, Bengaluru 560001, India

rotational diffusion equation is extended to an ellipsoid [5]. Several important assumptions of the SED's theory [6] must be tested in the case of the solute-solvent interactions on a microscopic scale molecule, stick and slip boundary conditions parameters on the molecular scale and rotational relaxation times in the solvent on the molecular scales. These assumptions strongly affect the solute-solvent interactions. A number of investigations have dealt with the study of the dependence of the rotational reorientation times [7–12] on the nature of the solvent, solute size, shape, charges on it, solvent temperature, pressure and solvent composition in binary mixtures to obtain a much better insight into the molecular rotation dynamics.

Molecule rotating in solution experience frictions because of its continuous interactions with its surrounding media and this has been the motivating factor to carry out the experimental rotational reorientation times measurements in solutions. How is this friction modeled? The general approach has been to treat the solute molecule as an ellipsoid moving in a continuous, homogeneous medium characterized by its macroscopic properties such as dielectric constant and viscosity. The friction has both mechanical and dielectric origins. Mechanical friction is modeled by hydrodynamics theories and the dielectric friction by different continuum theories [13–15]. The mechanical and dielectric friction contributions to the friction are non-separable because of the electrohydrodynamic coupling [16]. According to experimentalists, the non-separability of the total friction ($\zeta_{total}$) can be written as a contribution of mechanical ($\zeta_{MeF}$) and dielectric ($\zeta_{DiF}$) components

$$\zeta_{total} = \zeta_{MeF} + \zeta_{DiF} \tag{1}$$

However, elaborate examinations of rotational diffusions have shown the existence of origin of another drag regarding a rotating probe molecule because of specific solvent interactions like H bonding among the solute-solvent molecules. Such hydrogen bonding formation depends on the substituted functional groups of the solute molecules and the hydrogen bonding solvent molecules [17–22]. Under such conditions, the longer reorientation time is noticed, as a result of an increase in adequate rotating probe size. A number of investigations on dielectric friction have appeared in the literature [23–35] among which three theories are very important. The first one proposed by Nee and Zwanzing [NZ] [21] treats the solute as a point dipole rotating in a spherical cavity and solvent as a continuum dielectric medium. Second is a semi-empirical approach, which is proposed by van der Zwan and Hynes [24] in which fluorescence Stokes shift of the solute in the solvent media is related to the dielectric friction. The third model proposed by Alavi and Waldeck [27] is analogous and an extension to the NZ model wherein the dielectric friction is determined by treating solute as the arbitrary distribution of point charges. In this study, we wish to validate mechanical and dielectric frictional theories. We have chosen two solvents DMSO and Octanenitrile as their viscosities are similar and dielectric being different, to understand the variation in friction experienced by 7-DHB laser dye [36], when macroscopic solvent viscosity parameter is varied by varying the temperature.

## Materials and Experimental Methods

### Materials

The laser dye 7-[diethylamino]-2H-1-benzopyran-2-one: (7-DHB) was purchased from Exciton Company USA (with 98% purity) and used without further purification. Optimized geometry of studied dye molecular structure is shown in Fig. 1. The solvents DMSO and octanenitrile are commercially available from S-D Fine Chemicals Ltd., India is of the spectroscopic grade and used without further dilution. All the measurements measured at 298–343 ± 1 K and the concentration of the solution was maintained in the range of $10^{-5}$–$10^{-6}$ M.

### Experimental Methods

The steady-state absorption spectrum of the probe was recorded using a Shimadzu UV-1800 spectrophotometer with 1.0-nm resolution. The steady-state fluorescence spectrum of the probe was recorded using spectrofluorophotometer (Hitachi, model F-2700). Excitation and emission bandpass range from 0 to 10 nm and the photomultiplier voltage (PM) was set to 400 V depending on the fluorescence yield of the probe.

The Fluorescence anisotropy occurs as a result of the photo selection of fluorophore in the direction of the polarization of the excitation source. Fluorescence anisotropies were measured with exciting polarizer light in the Z-direction (laboratory frame) and detecting the components of fluorescence intensity polarized along with the Z and Y directions employing a Hitachi F-2700 spectrofluorophotometer, with polarizer accessories (Hitachi Model 650–0155 and 650–0156). The fluorescence intensity component polarized along the Z-direction is referred to as parallel ($I_{\|}$) and that polarized along the Y direction is called the perpendicular component ($I_{\perp}$). The steady-state Fluorescence anisotropy $< r >$ is characterised by [37].

$$< r >= \left[ \frac{I_{\|} - G_0 I_{\perp}}{I_{\|} + 2G_0 I_{\perp}} \right] \tag{2}$$

where '$G_0$' is a correction factor term. It is measured by using horizontally excitation polarized light intensity and horizontal and vertical polarization intensity of the emitted light. The $G_0$ correction factor term is given by $G_0 = \left[ \frac{I_{HV}}{I_{HH.}} \right]$

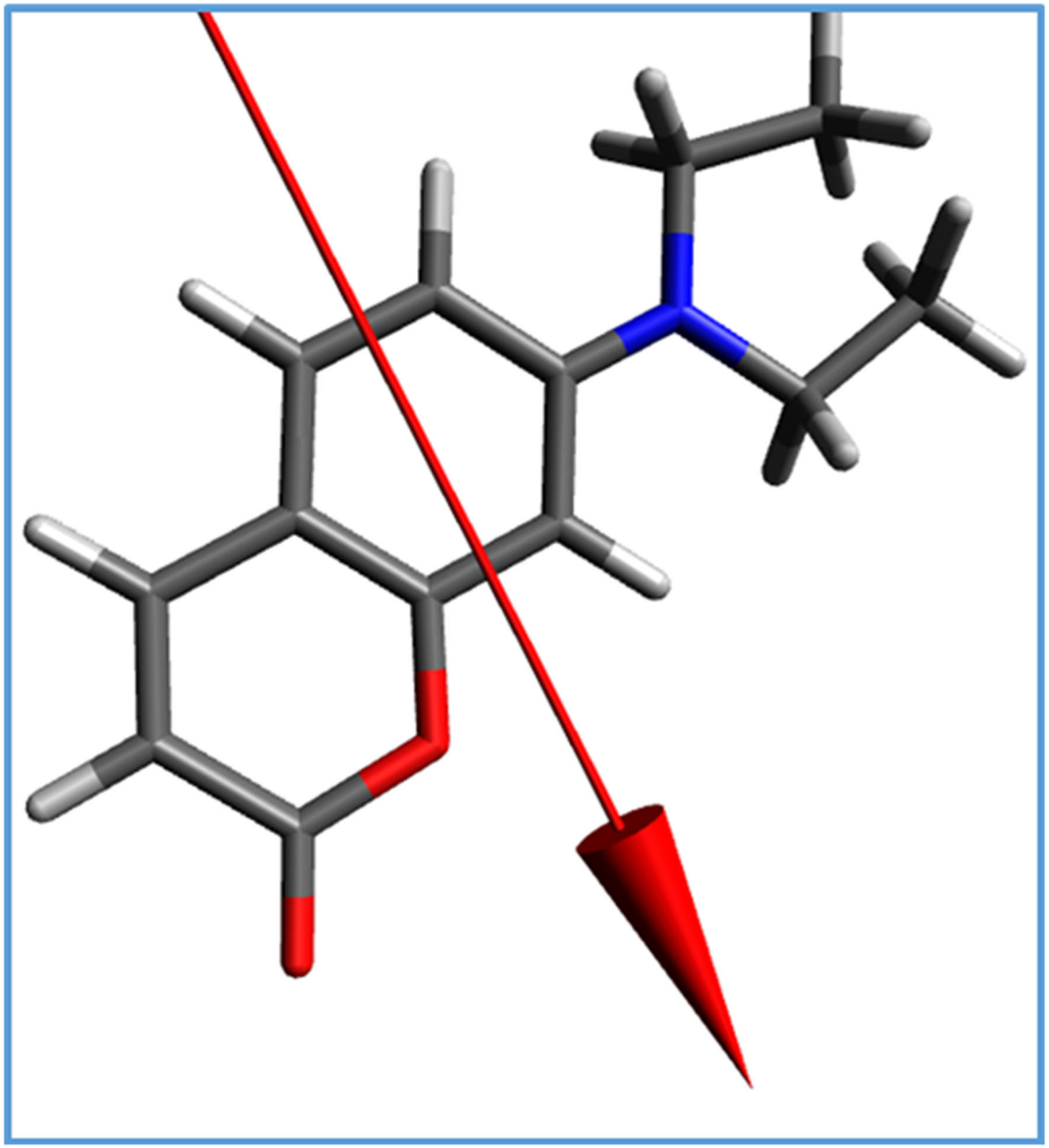

**Fig. 1** Optimized molecular structure of 7-DHB laser dye used in the study

Fluorescence decay of 7-DHB dye molecule in solvents (Fig. 2) was recorded using picosecond laser as an excitation source and a time-correlated single photon counting (TCSPC) technique (Edinburgh Instruments, Model: FSP920) along with Hamamatsu PMT is used for fluorescence detector. The excitation source of 408 nm wavelength diode laser (< 100 ps, 1MHZ) was used. The device response function was ~260 ps at FWHM. Fluorescence decays measured with an excitation beam of vertically polarized and fluorescence was collected at the magic angle ($54.7^0$). For all fluorescence detection, the spectral bandwidth is kept at ~7.0 nm. Data analysis of fluorescence decay was done by nonlinear least square and iterative reconvolution methods. The fluorescence decay curve analysis was performed by using the software IBH (DAS-6) based on reconvolution technique.

The rotational reorientation times ($\tau_r$) is found from experimentally measured using the relation [37] by

$$\tau_r = \tau_f / \left[ \left( \frac{r_o}{\langle r \rangle} \right) - 1 \right] \quad (3)$$

where $\tau_f$ – is fluorescence lifetime and $r_o$ – is limiting anisotropy found in the frozen state of the molecules. $r_o$ - measured by dissolving the probe molecule in glycerol and cooling the solution to a temperature below −18 °C.

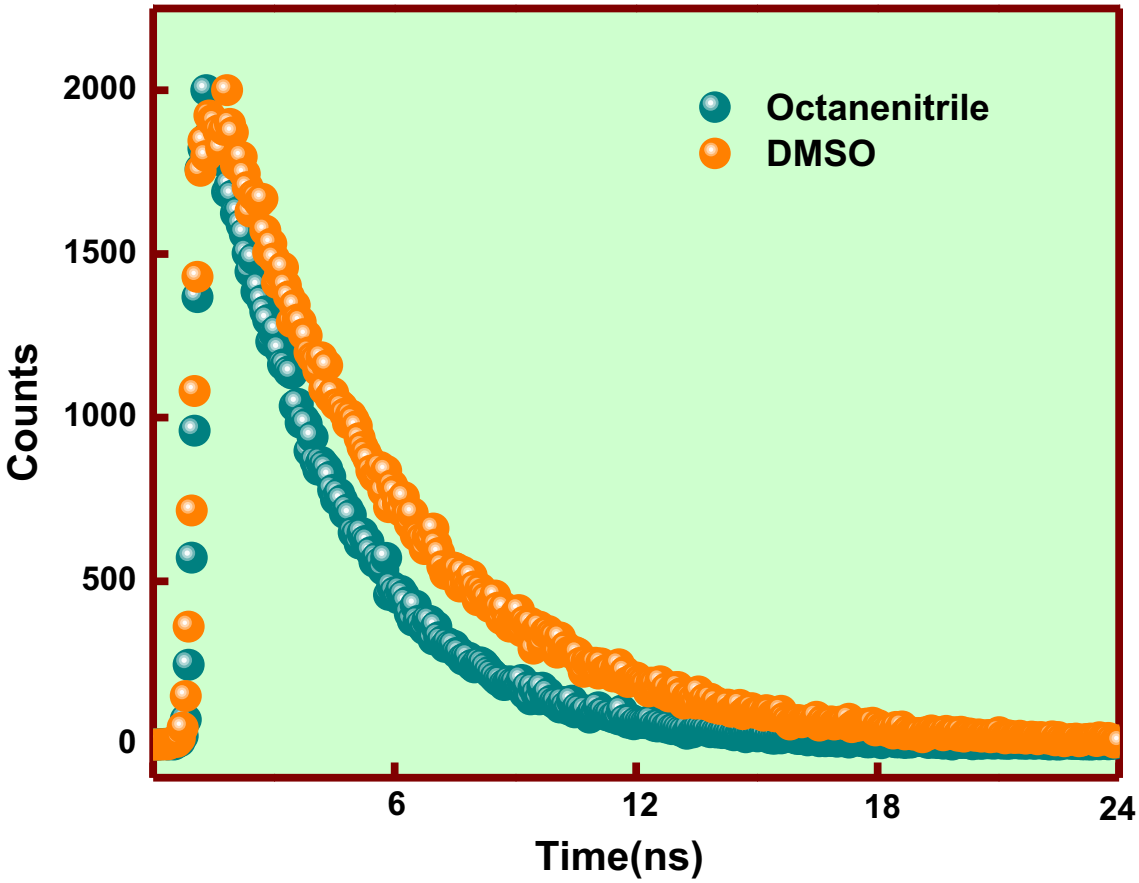


**Fig. 2** Fluorescence decay curve of 7-DHB in DMSO and Octanenitrile solvents at 298 K

## Computational Techniques

The Time-Dependent Density Functional Theory [TD-DFT] calculations were carried out for the probe using the GAMESS software package [38–40]. Ground state optimized geometry were computed using TD B3LYP/6-31G basis set. To incorporate both dynamical and non-dynamical correlations effects, the most familiar ab-initio methods were used. Vertically excited zero-zero singlet states were also computed using the same basis set.

## Results and Discussion

### Computational Results

Initially, optimized geometry was computed using QM-AM1 method. For 7-DHB diethylamine (-N-$CH_3$) group bond length, for atom N-12 and C-13 is 1.4866 Å and for atom N-12 and C-15 is 1.4956 Å. In DMSO and octanenitrile solvents, HOMO-LUMO is completely localized over the entire molecule expect on diethyl amine group. Parameters such as partial charges,

**Table 1** Steady state anisotropy <r>, fluorescence life time ($\tau_f$) and rotational reorientation

| Temperature/ K | Viscosity η/ mPa S[a] | Anisotropy <r> | Fluorescence lifetime $\tau_f$/ns | Rotational reorientation time $\tau_r$/ps |
|---|---|---|---|---|
| 298 | 1.98 | 0.021 | 3.73 | 199.82 |
| 303 | 1.83 | 0.019 | 3.67 | 176.98 |
| 313 | 1.52 | 0.016 | 3.51 | 141.46 |
| 323 | 1.21 | 0.011 | 3.47 | 94.95 |
| 333 | 0.91 | 0.009 | 3.36 | 74.85 |
| 343 | 0.60 | 0.005 | 2.81 | 34.44 |

Time ($\tau_r$) of 7-DHB in DMSO as a function of temperature

[a] - viscosity data from extrapolation data of Ref. 36

**Table 2** Steady state anisotropy <r>, fluorescence life time ($\tau_f$) and rotational reorientation time ($\tau_r$) of 7-DHB in Octanenitrile as a function of temperature

| Temperature/ K | Viscosity η/ mPa S[a] | Anisotropy <r> | Fluorescence lifetime $\tau_f$/ns | Rotational reorientation time $\tau_r$/ps |
|---|---|---|---|---|
| 298 | 1.65 | 0.018 | 3.86 | 175.90 |
| 303 | 1.54 | 0.014 | 3.83 | 134.39 |
| 313 | 1.31 | 0.012 | 3.83 | 114.61 |
| 323 | 1.08 | 0.011 | 3.81 | 104.25 |
| 333 | 0.85 | 0.006 | 3.80 | 56.02 |
| 343 | 0.62 | 0.002 | 3.77 | 18.35 |

[a] - viscosity data from extrapolation data of Ref. 36

coordinates, dipole moment, etc., of the probe molecule in the excited state were obtained from the SCF density matrix.

### Hydrodynamic Theory

Mechanical friction is modeled by hydrodynamics theories [13]. According to the SED theory, the $\tau_r$–rotational reorientation time relates to η-viscosity of the solvent, k – Boltzmann constant, V- is the van der Waals volume of the probe, T – absolute temperature, f – shape factor, which is given by the equation

$$\tau_r = \left[ \frac{\eta V}{kT} fc \right] \tag{4}$$

To calculate the rotational reorientation times of probe molecules by applying SED theory the shape factor, stick and slip boundary conditions parameters are determined as follows: In accordance with van der Waals increment method [41], the probe molecular volume of 7-DHB was found to be 203.5Å$^3$. The thickness of the probes C = 1.9 Å for aromatic molecules was taken as half-axis proposed by Fleming et al. [42]. The longest axis (2a) of the probe molecules was taken as the end to end distance. The short in-plane axes (2b) have been found by employing the relation $V = \left[\frac{4\pi}{3} abc\right]$ where V- is the probe volume, the half-axis being a, b and c. The determined van der Waals, axial radii parameters of the probe molecules are 9.33 Å (=a), 2.7 Å (=b) and 1.9 Å (=c). From the estimation of axial radii's, 7-DHB probe is modeled as an asymmetric ellipsoid.

The coefficients of friction along a, b and c axis with stick boundary condition parameters were found by interpolation of the numerical data of Small and Isenberg [43]. Slip boundary condition parameters were found by numerical data of Hochstrasser et al. [44]. The diffusion coefficients were determined by the relation of the frictional coefficients $\zeta_i$ of the form $D_i = KT/\zeta_i$ by which the rotational reorientation times are determined using the Eq.1 assuming transition dipole moment is along longest axes

$$\tau_r = \frac{1}{12} \left[ \frac{4D_1 + D_2 + D_3}{D_1D_2 + D_2D_3 + D_3D_1} \right] \tag{5}$$

Where $D_1$, $D_2$ and $D_3$ are diffusion coefficients along long, short and out-of-plane axes respectively. The rotational reorientation times of the dye 7-DHB molecule with a stick and slip boundary conditions (using eq.6) values are found to be176.38 ps and 105.0 ps. Also, f- shape factor (f) and $C_{slip}$ of laser dye 7-DHB are 3.565, 0.595 respectively.

Steady-state fluorescence anisotropy (<r>), fluorescence lifetime ($\tau_f$) and rotational re-orientation times ($\tau_r$) of 7-DHB obtained experimentally with a change in temperature, are tabulated in Tables 1 & 2. It can be inferred that, fluorescence lifetimes of the probe marginally higher in DMSO and Octanenitrile. The $\tau_f$ value range from 2.81–3.73 ns and 3.77–3.86 in DMSO and Octanenitrile respectively. Limiting anisotropy ($r_0$) values for 7-DHB value is 0.413. Average values of fluorescence anisotropy's (<r>) are 0.0135 and 0.0105 in DMSO and Octanenitrile respectively. From the values of $r_0$, <r> and $\tau_f$, the rotation reorientation times $\tau_r$ were determined (using Eq.3). The $\tau_r$ values decrease in both the solvents with an increase in temperature. $\tau_r$ values in DMSO are larger than Octanenitrile by a factor of 1.136, which indicates that 7-DHB laser dye is experiencing higher friction in DMSO to some extent than octanenitrile. Using Tables 1 and 2, data for 7-DHB molecule, the plots $\tau_r$ v/s η/T least square fitting was performed in both the solvents. A negative intercept of −22.18 ps in DMSO and − 41.25 ps in octanenitrile is noticed, which represents the non-linear relationship between $\tau_r$ and η/T. So, logarithmic fits of $\tau_r$ and η/T were performed for both solvents, obtained relationship results are tabulated in Table 3. From Table 3, it can be found data between $\tau_r$ and η/T to be nearly linear. A graph of $\tau_r$ v/s η/T is plotted for 7-DHB in DMSO and octanenitrile solvents along with slip and stick lines are shown in Fig. 3.

**Table 3** Relationship between $\tau_r$ and η/T obtained from the logarithmic fits of the data for 7-DHB in a) DMSO and b) Octanenitrile

| Solute | DMSO | Octanenitrile |
|---|---|---|
| 7-DHB | $(0.411 \pm 0.09)\left(\frac{\eta}{T}\right)^{0.97}$ | $(0.639 \pm 0.06)\left(\frac{\eta}{T}\right)^{0.99}$ |

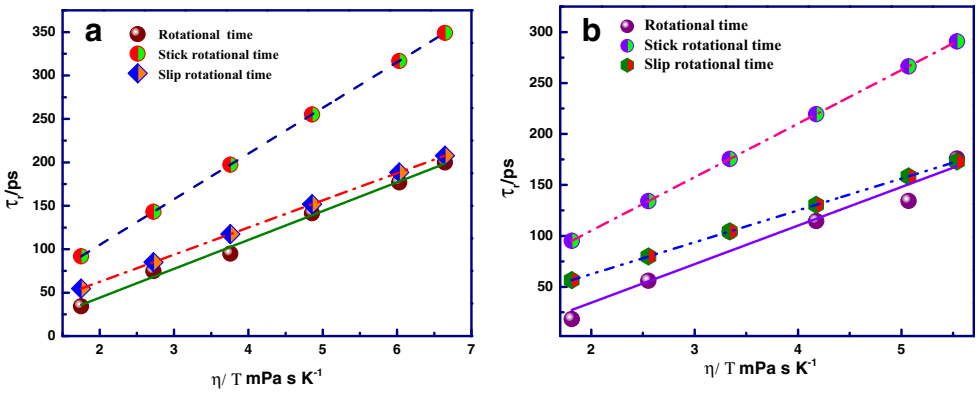


**Fig. 3** Plots of rotational time as a function of viscosity/Temperature of 7-DHB in (**a**) DMSO (**b**) Octanenitrile with the theoretical stick and slip lines

Rotational reorientation times ($\tau_r$) are calculated with slip (15.81 x η/T) and stick (26.56 x η/T) boundary conditions parameters for the studied probe. The difference between experimental rotational time and slip rotational times are in the range of about 9% - 21% for DMSO and 3% - 39% for octanenitrile solvents. From the calculation of the hydrodynamic friction amounts to 20% and 3% of the observed friction for 7-DHB in DMSO and octanenitrile solvents respectively. A graph $\tau_r$ v/s η/T is plotted in DMSO and octanenitrile solvents along with slip and stick lines Fig. 3. The experimentally observed reorientation times for 7-DHB laser dye lies below slip and stick boundary conditions lines in both solvents (Fig. 3). The $\tau_r$ values for 7-DHB in DMSO are observed to be slightly near with slip rotational reorientation time as predicted by the hydrodynamic theory. It is interesting to note that experimental and theoretical slip $\tau_r$ values converge for higher temperature for both solvents. Generally, dielectric friction is experienced in case of polar probe rotating in a polar solvent. However, mechanical friction of 3% - 20% is observed for the probe in solvents of the total friction. Table 3 implies that; the probe is experiencing 24% more friction in DMSO compared to octanenitrile solvent. The observed deviations from the experimental results with that predicted SED theory have been quantitatively explained using different dielectric theories.

**Table 4** Solvent Dielectric and related properties of solvents used in this study as a function of Temperature

| Solvent | Temperature/ K | $\varepsilon_0$ [a] | $\varepsilon_\infty$ [b] | $\tau_D$/ ps | A X $10^3$ / ps $K^{-1}$ |
|---|---|---|---|---|---|
| DMSO | 298 | 48.9 | 3.9 | 24 | 12.3 |
| | 303 | 47.4 | 3.3 | 21 | 9.03 |
| | 313 | 44.5 | 2.3 | 15 | 4.51 |
| | 323 | 41.5 | 1.4 | 9.0 | 1.88 |
| | 333 | 38.6 | 24 | 3.0 | 0.44 |
| | 343 | 35.7 | 0.4 | 1.3 | 0.33 |
| Octanenitrile | 298 | 13.0 | 2.72 | 31.4 | 2.92 |
| | 303 | 12.4 | 2.35 | 29.4 | 2.51 |
| | 313 | 11.2 | 1.71 | 25.5 | 1.83 |
| | 323 | 10.0 | 1.16 | 21.6 | 1.32 |
| | 333 | 8.80 | 0.72 | 17.7 | 0.95 |
| | 343 | 7.60 | 0.38 | 13.7 | 0.68 |

[a, b] Dielectric parameters and $\tau_D$ values are obtained from interpolation/ extrapolation data Ref. 36

## Dielectric Friction

Two Semi-empirical methods proposed by Nee-Zwanzig (NZ) [21] and Zwan-Hynes (ZH) [24] models and the third model proposed by Alavi and Waldeck [27] by treating solute as the arbitrary distribution of point charges have been employed to calculate the contribution of dielectric frictions

## Nee-Zwanzig (NZ) Model

When the molecule starts rotating, surrounding media cannot polarise instantaneously and keep in phase with the new orientation of the probe molecule, this lag exerts a retarding force giving rise to rotational dielectric friction on the probe. NZ model solvent is regarded as an extended dielectric media described by a frequency dependants of dielectric constants and probe to be a point dipole embedded in a cavity of radius 'a'. If, $\varepsilon_0$ – zero frequency dielectric constants and $\varepsilon_\infty$ - dielectric constants at high-frequency of the solvent medium, $\mu_e$ - is the excited state dipole moment and $\tau_D$ – Debye relaxations time of the medium. The dielectric friction ($\tau_{DF}$) of the probe at the limit of zero frequency is followed by an equation as

**Table 5** Excited state dipole moments obtained from the slope of the $\tau_{DF}$ v/s A using NZ theory

| Solvent | Slope | Intercept | Dipole Moment | |
|---|---|---|---|---|
| | | | a = 3.65 Å | a = 9.33 Å |
| DMSO | 6.96355 | 72.90972 | 64.86 | 28.41 |
| Octanenitrile | 24.4309 | 31.70013 | 121.49 | 53.22 |

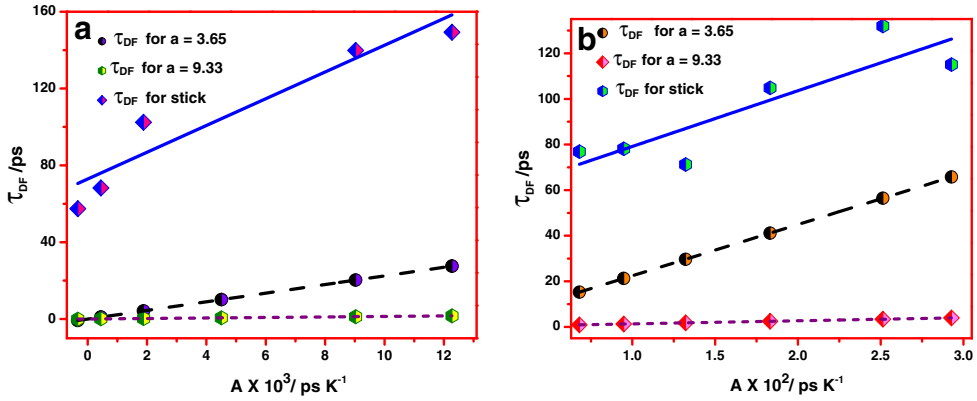


**Fig. 4** Rotational time due to dielectric friction $\tau_{DF}$ of 7-DHB ($\tau_{DF}= \tau_r^{Obs} - \tau_r^{Stick}$ ) as a function of A in (**a**) DMSO (**b**) Octanenitrile

$$\tau_{DF} = \left[ \frac{\mu_e^2}{9a^3KT} \frac{(\varepsilon_\infty + 2)^2(\varepsilon_0 - \varepsilon_\infty)}{(2\varepsilon_0 + \varepsilon_\infty)^2} \tau_D \right] \quad (6)$$

$$A = \frac{(\varepsilon_\infty + 2)^2(\varepsilon_0 - \varepsilon_\infty)}{(2\varepsilon_0 + \varepsilon_\infty)^2} \tau_D \quad (7)$$

The $\tau_D$ values and static dielectric properties of studied solvents are tabulated in Table 4. obtained from the literature [36]. The dipole moments in an excited state of the probe is 11.651D were determined by using Lippert-Mataga eq. [10] and shown in Table 5. Two sets of $a_0$ values for a given solute are employed to determine the contributions of dielectric friction which serves as two maximum limits. The first set of values of $a_0 = 3.65$ Å found from the van -der-Waals volumes, considering the probe as a spherical molecule and the second set of value are obtained from the half-length of the longest-axes of which values are $a_0 = 9.33$ Å for 7-DHB in both the solvents. To examine the experimentally obtained dielectric friction with that of theoretically calculated dielectric friction, the contribution of $\tau_{DF}$ was calculated with the experimental rotational reorientation time using the relation: $\tau_{DF} = \tau_r^{Expt} - \tau_r^{stick}$ and $\tau_{DF} = \tau_r^{Expt} - \tau_r^{DKS}$ for the probe, where $\tau_r^{Expt}$ – is the experimentally determined rotational reorientation time and $\tau_r^{stick}$ and $\tau_r^{DKS}$ – are the theoretical determined rotational reorientation time as per SED and CDKS theory respectively. A plot of $\tau_{DF}$ v/s A was plotted for the probe (Fig. 4), where

From Fig. 4, it can be inferred that the contribution of dielectric friction by NZ theory underestimates with the experimental values for both maximum limits in DMSO and octanenitrile solvent. That had been revealed in unrealistic large dipole moments values, obtained from the slopes of $\tau_{DF}$ v/s A plots (Table 5). From Table 4, the 'A' values are 1–4.2 times greater in DMSO than Octanenitrile, as per NZ model the $\tau_{DF}$ contribution be higher magnitude in DMSO. This may be probably the reason for higher dielectric friction consequently slower rotation and higher rotational reorientation time in DMSO than Octanenitrile experienced by 7-DHB probe.

## Van der Zwan Hynes (ZH) Model

An advanced theory over the semi-empirical NZ theory for determining dielectric friction was proposed by van der Zwan and Hynes [45]. ZH theory describes dielectric friction experienced by the probe in terms of solute response to a solvent. The dielectric friction experienced by the probe in a solvent is related to the solvatochromic Stoke's shift and solvation times ($\tau_s$). It is given by

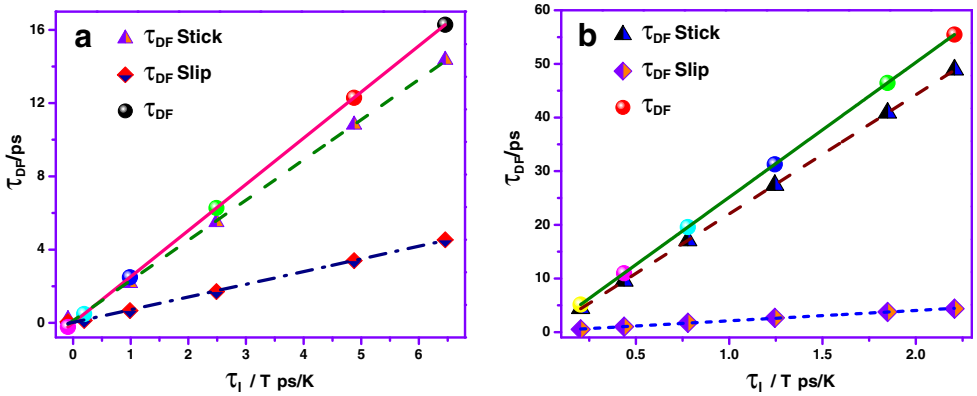


**Fig. 5** Rotational time due to dielectric friction $\tau_{DF}$ ($\tau_{DF}= \tau_r^{Obs} - \tau_r^{Stick}$ and $\tau_{DF}= \tau_r^{Obs} - \tau_r^{slip}$ ) as a function of $\tau_l$ / T for 7-DHB in (**a**) DMSO and (**b**) Octanenitrile

**Table 6** Slopes, intercepts and $\mu^2/\Delta\mu^2$ values obtained from the plot of $\tau_{DF}$ v/s $\tau_l/T$ using the ZH theory in the solvents

| Solvent | Slope | Intercept | $\frac{\mu^2}{\Delta\mu^2}$ |
|---|---|---|---|
| DMSO | 2.52146 | −5.32907 | 0.463429 |
| Octanenitrile | 25.13866 | −1.77636 | 4.620337 |

$$\tau_{DF} = \left[\left(\frac{\mu^2}{\Delta\mu^2}\right)\frac{hc\Delta\nu}{6KT}\ \tau_s\ \right] \quad (8)$$

Where, μ – dipole moment, h - Planck's constant, c - velocity of light in vacuum, $\tau_s$–solvation time, and Δν- Stoke's shift (energy difference between 0 and 0 transition for excitation and 0–0 emission in a given solvent), Δμ – the difference between excited and ground state dipole moment and K-Boltzmann constant. Numerous studies [46–53] on solvation dynamics imply that longitudinal relaxation time of the solvent $\tau_l = \tau_D$ ($\varepsilon_\infty/\varepsilon_0$) is closely related to solvation time and is nearly independent properties of the probes. So $'\tau_l'$ may be replaced by solvation time. Using the Eq. 8 (ZH model) the dielectric friction ($\tau_{DF}$) contributions were calculated by, employing stokes shift values as 3862.74 $cm^{-1}$ and 3851.1 $cm^{-1}$. The $\tau_{DF}$ values found from ZH model and experimental results are plotted as a function of $\tau_l/T$ as shown in Fig. 5. From Fig. 5. It can be noted that the dielectric friction calculated theoretically by ZH model underestimates the observed experimental dielectric friction for $\tau_{DF} = \tau_r^{Expt} - \tau_r^{slip}$ and is nearly equal $\tau_{DF} = \tau_r^{Expt} - \tau_r^{stick}$, it is exciting to note that $\tau_{DF} = \tau_r^{Expt} - \tau_r^{stick}$ are nearly equal for rotational reorientation at lower temperatures, but it deviates slightly at a higher temperature. The $\frac{\mu^2}{\Delta\mu^2}$ values are determined by the slopes obtained from $\tau_{DF}$ v/s $\tau_l/T$ plots and results are tabulated in Table 6 along with experimentally determined values. The determined $\frac{\mu^2}{\Delta\mu^2}$ values are higher by a factor of 11.67 and 1.17 for DMSO and octanenitrile. For the $\frac{\mu^2}{\Delta\mu^2}$ difference values obtained using ZH model in DMSO and octanenitrile, it may be explained by Stoke's shift values being larger compared to the actual values and that might be the cause $\frac{\mu^2}{\Delta\mu^2}$ values that are calculated from the $\tau_{DF}$ v/s $\Delta\nu\tau_l$ are smaller compared to the calculated ones? So, solvatochromic Stoke's shift values itself cannot account for such a difference among the experimental and theoretical results. Evidently, both NZ and ZH models also fail to explain the examined behavior, even in the qualitative way.

### Alavi-Waldeck (AW) Model

To enhance the microscopic effect on dielectric frictions for polar solutes and to describe dielectric frictions experienced by it when embedded in polar solvents, Alavi-Waldeck et al. (AW model) [29, 54–58] proposes that it is applied point charge distributions than, the extended charge distributions which contribute significantly to dielectric friction in addition

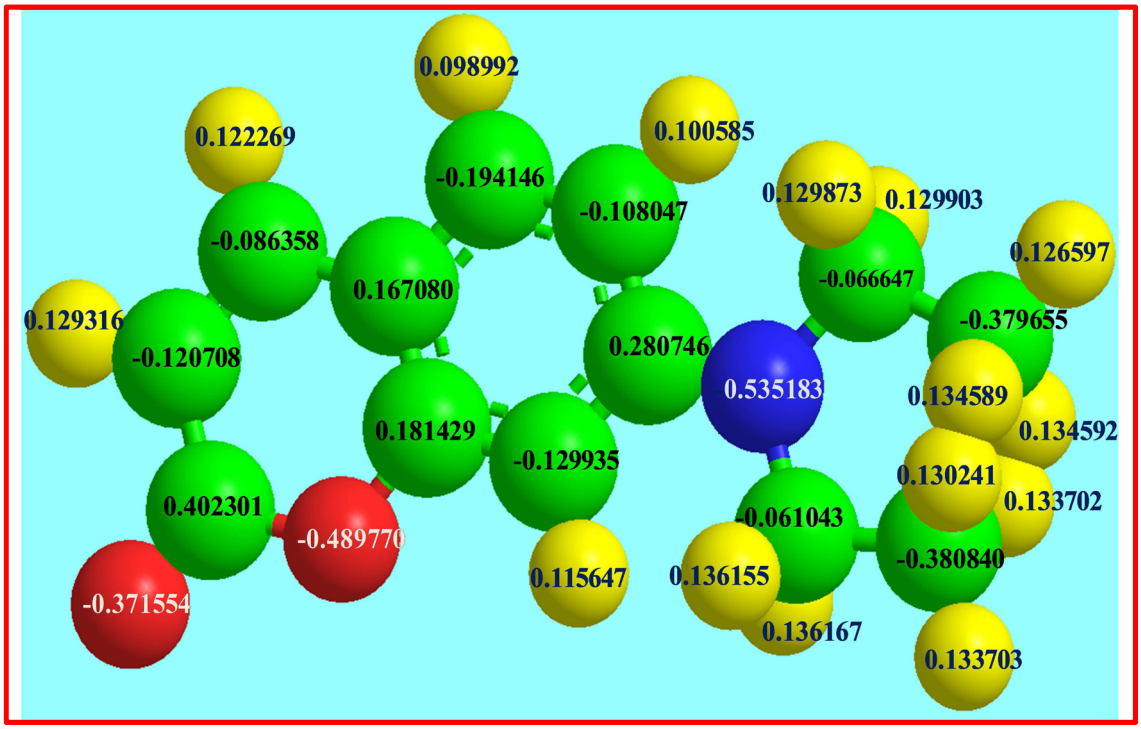


**Fig. 6** Partial charge distribution in the excited state of 7-DHB molecule

**Table 7** Cartesian coordinates and partial charges on the atoms in the excited state of 7-DHB probe

| Atom | X | Y | Z | Partial charges |
|---|---|---|---|---|
| C(1) | −3.8816 | −0.9077 | −0.00070 | 0.402301 |
| C(2) | −4.1809 | 0.4931 | −0.00009 | −0.120708 |
| C(3) | −3.2458 | 1.5173 | 0.000270 | −0.086358 |
| C(4) | −1.7881 | 1.1796 | 0.000160 | 0.167082 |
| C(5) | −1.4292 | −0.1847 | −0.000200 | 0.181429 |
| O(6) | −2.3358 | −1.2167 | −0.000500 | −0.489771 |
| C(7) | −0.0493 | −0.5847 | −0.000200 | −0.129935 |
| C(8) | 0.9732 | 0.3834 | 0.000089 | 0.280746 |
| C(9) | 0.6322 | 1.7559 | 0.000471 | −0.108047 |
| C(10) | −0.7435 | 2.1222 | 0.000512 | −0.194146 |
| O(11) | −4.6002 | −1.9306 | 0.000143 | −0.371554 |
| N(12) | 2.3976 | −0.0716 | −0.000002 | −0.535183 |
| C(13) | 3.3793 | 1.0352 | −0.000302 | −0.066647 |
| C(14) | 4.8971 | 0.7803 | −0.000912 | −0.379655 |
| C(15) | 2.6269 | −1.5442 | 0.000381 | −0.061043 |
| C(16) | 4.0540 | −2.1234 | 0.000771 | −0.380842 |
| H(17) | −5.2493 | 0.7254 | 0.000231 | 0.129316 |
| H(18) | −3.5487 | 2.5646 | 0.000752 | 0.122269 |
| H(19) | 0.1293 | −1.6563 | −0.000622 | 0.115647 |
| H(20) | 1.3747 | 2.5476 | 0.000782 | 0.100585 |
| H(21) | −0.9953 | 3.1864 | 0.000831 | 0.098992 |
| H(22) | 3.1294 | 1.6667 | 0.879193 | 0.129873 |
| H(23) | 3.1287 | 1.6667 | −0.879711 | 0.129903 |
| H(24) | 5.3840 | 1.7701 | −0.001512 | 0.126597 |
| H(25) | 5.2433 | 0.2447 | −0.89621 | 0.134592 |
| H(26) | 5.2441 | 0.2453 | 0.894265 | 0.134589 |
| H(27) | 2.0955 | −1.9495 | −0.88282 | 0.136155 |
| H(28) | 2.0952 | −1.9493 | 0.883576 | 0.136167 |
| H(29) | 3.9486 | −3.2211 | 0.001353 | 0.130241 |
| H(30) | 4.6291 | −1.8485 | 0.895853 | 0.133702 |
| H(31) | 4.6292 | −1.8494 | −0.89454 | 0.133703 |

to that of dipole moment and higher-order moments of the solute, this is major difference in NZ and AW. AW model adequately emphasizes the fact that solute with permanent dipole should experience less dielectric friction compared with no permanent dipole. The coefficient of frictions according to AW theory is given by

$$\zeta_{DF} = \frac{8}{a}\frac{(\varepsilon_0-1)}{(2\varepsilon_0+1)^2}\tau_D \times \sum_{j=1}^{N}\sum_{i=1}^{N}\sum_{L=1}^{L_{max}}\sum_{M=1}^{L}\left(\frac{2L+1}{L+1}\right)\frac{(L-M)!}{(L+M)!} \times M^2 q_i q_j \times \left(\frac{r_i}{a}\right)^L\left(\frac{r_j}{a}\right)^L \times P_L^M(cos\,\theta_i)P_L^M(cos\,\theta_j)\cos M\varnothing_{ij}. \quad (9)$$

Where, $q_i$ –the partial charge on an $i^{th}$ atom with ($r_i$, $\theta_i$, $\varnothing_i$) as spherical coordinates, $\varnothing_{ji} = \varnothing_j - \varnothing_i$, N – the number of atoms in the probe, a – cavity radius, L – is a spatial variation of distributed charge at the cavity surface and $P_L^M(x)$ – associate Legendre's polynomial. In AW model to determine dielectric friction, sums of associated Legendre polynomials are used, in order to describe the electrostatic field of the probe due to partial charge distribution over the surface of the spherical Onsager cavity. $L_{max}$ – is the limited value of L below which the solvent respond to the solutes spatial variation of distributed charge. Limited value $L_{max}$ is dependent on the relative size of the solvent and probe. It is given by

$$L_{max} = 2\left[\frac{(r_{solute}+r_{solvent})^2}{(r_{solvent})^2}\right] \quad (10)$$

Where, $r_{solute}$ – solute radii and $r_{solvent}$ – solvent radii.

The dielectric friction in the AW model is dependent on solvent dielectric properties similar to the NZ equation for a point dipole but has a different electrical properties dependence of the probe. Using eq.10 dielectric friction experienced by the probe in solvents was calculated. Partial charges (Fig. 6), coordinates of excited atoms of the probe is described in computational techniques section (Table 7). Using van der Waals volume, radii found to be, $r_{solute} = 9.33$ Å which is half the length of the longest axis, $r_{solvent} = 2.64$ Å for DMSO and $r_{solvent} = 3.29$ Å octanenitrile solvents, for $L_{max}$ values using Eq. 10 are found to be 42 in DMSO and 30 in octanenitrile. Diffusion coefficients ($D_i$) along each axis were calculated from friction coefficients $\zeta_i$ using the relation $D_i = kT/\zeta_i$ and rotational reorientation times is calculated using the eq. 5

As the charges are placed near to the boundary of the spherical cavity, the AW model is very sensitive to the cavity radius 'a' for calculating rotational reorientation times. A wide range of 'a' closer to half-length of the longest axis of the probe molecule has been chosen. For different solvent-probe combinations, 'a' value is varied till calculated rotational reorientation time at each temperature 'matches with the experimental one. The maximum difference among the longest axial and best-fit cavity radius is 23%. The ratio of calculated reorientation time to the observed are more are less nearly equal to one. Average of 'a' value is taken as the best fit radius of the cavity. The best-fit radius of the cavity is 9.59 Å in DMSO and 9.88 Å in octanenitrile. Experimental and theoretical values are in good agreement within 10% in DMSO and 30% in octanenitrile. AW model is adequate to describe friction experienced by the probe at particular temperatures in a given solvent.

## Conclusions

Rotational reorientation time of 7-DHB laser dye is measured in two non-associative solvents, DMSO and Octanenitrile by varying the temperature. In DMSO rotational reorientation times are observed to be slightly near with super slip rotational reorientation time as predicted by the hydrodynamic theory.

SED theory couldn't explain deviations from experimental results for probe molecule and the observed deviations from the experimental results with that predicted SED theory have been quantitatively explained using different dielectric theories. Dielectric friction models NZ and ZH which treats the probe as a point dipole, couldn't describe even qualitatively the observed trend. NZ theory underestimates with the experimental values for both maximum limits in solvents. Though ZH model explains through the stick dielectric behavior, it fails to explain even qualitatively. Alavi-Waldeck treats extended charge distributions to explain the observed behavior in a qualitatively way. It can be concluded that dielectric friction theories using point dipole moment fail to model both in associative and non-associative solvents even in qualitatively way, however, extended charge distribution model works at least in non-associative solvents qualitatively.

## References


1. Mali KS, Dutt GB, Mukherjee T (2008) Rotational diffusion of a nonpolar and a dipolar solute in 1-butyl-3-methylimidazolium hexafluorophosphate and glycerol: interplay of size effects and specific interactions. J Chem Phys 128:054504–1-054504-9. https://doi.org/10.1063/1.2827473
2. Tao T (1969) Time-dependent fluorescence depolarization and Brownian rotational diffusion coefficients of macromolecules. Biopolymers. 8:609–632
3. Einstein A (1956) Investigations in Theory of Brownian Motion. Dover, New York
4. Kubinyi M, Grofcsik A, Pápai I, Jones WJ (2003) Rotational reorientation dynamics of nile blue a and oxazine 720 in protic solvents. Chem Phys 286:81–96. https://doi.org/10.1016/S0301-0104(02)00908-4
5. Zhou P, Song P, Liu J, Shi Y, Han K, He G (2008) Rotational reorientation dynamics of oxazine 750 in polar solvents. J Phys Chem A 112:3646–3655. https://doi.org/10.1021/jp7120998
6. Raikar US, Renuka CG, Nadaf YF, Mulimani BG, Karguppikar AM (2006) Rotational diffusion and solvatochromic correlation of coumarin 6 laser dye. J Fluoresc 16:847–854. https://doi.org/10.1007/s10895-006-0126-4
7. Gangamallaiah V, Dutt GB (2012) Rotational diffusion of nonpolar and ionic solutes in 1-Alkyl-3- methylimidazolium bis (trifluoromethylsulfonyl) imides: is solute rotation always influenced by the length of the alkyl chain on the imidazolium cation? J Phys Chem B 116:12819–12825. https://doi.org/10.1021/jp307959z
8. Prabhu SR, Dutt GB (2014) Rotational diffusion of nonpolar and charged solutes in propylammonium nitrate-propylene glycol mixtures: does the organized structure of the ionic liquid influence solute rotation? J Phys Chem B 118:2738–2745. https://doi.org/10.1021/jp501343k
9. Prabhu SR, Dutt GB (2014) Rotational diffusion of nondipolar and charged solutes in alkyl-substituted imidazolium triflimides: effect of C2 methylation on solute rotation. J Phys Chem B 118:9420–9426. https://doi.org/10.1021/jp5055155
10. Nadaf YF, Renuka CG, Raikar US (2013) Temperature-dependent reorientation dynamics of laser dyes in alkane and alcohol solvents. Can J Phys 91:677–681
11. Anirban Sharma, Pradip Kr. Ghorai (2018) Effect of alcohols on the structure and dynamics of [BMIM][PF6] ionic liquid: a combined molecular dynamics simulation and Voronoi tessellation investigation. J Chem Phys 148: 204514–1–204514–11. https://doi.org/10.1063/1.5008439
12. Nadaf YF, Renuka CG (2015) Analysis of rotational diffusion of coumarin laser dyes. Can J Phys 93:3–6
13. Dutt GB, Ghanty TK (2004) Rotational dynamics of nondipolar probes in butanols: correlation of reorientation times with solute-solvent interaction strengths. J Phys Chem A 108:6090–6095. https://doi.org/10.1021/jp048601q
14. Hay CE, Marken F, Blanchard GJ (2010) Solvent-dependent changes in molecular reorientation dynamics: the role of solvent-solvent interactions. J Phys Chem A 114:4957–4962. https://doi.org/10.1021/jp912217r
15. Jin H, Baker GA, Arzhantsev S, Dong J, Maroncelli M (2007) Solvation and rotational dynamics of coumarin 153 in ionic liquids: comparisons to conventional solvents. J Phys Chem B 111:7291–7302. https://doi.org/10.1021/jp070923h
16. Kumar PV, Maroncelli M (2000) The non-separability of dielectric and mechanical friction in molecular systems: a simulation study. J Chem Phys 112(12):5370–5381. https://doi.org/10.1063/1.481107
17. Prabhu SR, Dutt GB (2015) Rotational diffusion of charged and nondipolar solutes in ionic liquid-organic solvent mixtures: evidence for stronger specific solute-solvent interactions in presence of organic solvent. J Phys Chem B 119:10720–10726. https://doi.org/10.1021/acs.jpcb.5b06297
18. Dutt GB (2005) Molecular rotation as a tool for exploring specific solute-solvent interactions. Chem Phys Chem 6:413–418. https://doi.org/10.1002/cphc.200400337
19. Guo J, Han KS, Mahurin SM, Baker GA, Hillesheim PC, Dai S, Hagaman EW, Shaw RW (2012) Rotational and translational dynamics of rhodamine 6G in a pyrrolidinium ionic liquid: a combined time-resolved fluorescence anisotropy decay and NMR study. J Phys Chem B 116:7883–7890
20. Tiwari AK, Sonu SSK (2014) Effect of hydroxyl group substituted spacer group of cationic gemini surfactants on solvation dynamics and rotational relaxation of coumarin-480 in aqueous micelles. J Phys Chem B 118:3582–3592. https://doi.org/10.1021/jp4069703
21. Nee TW, Zwanzig R (1970) Theory of dielectric relaxation in polar liquids. J Chem Phys 52:6353–6363. https://doi.org/10.1063/1.1672951
22. Hu C, Zwanzig R (1974) Rotational friction coefficients for spheroids with the slipping boundary condition. J Chem Phys 60:4354–4357
23. Madden P, Kivelson D (1982) Dielectric friction and molecular reorientation. J Phys Chem 86:4244–4256. https://doi.org/10.1021/j100218a031
24. Van Der Zwan G, Hynes JT (1985) Time-dependent fluorescence solvent shifts, dielectric friction, and nonequilibrium solvation in polar solvents. J Phys Chem 89:4181–4188. https://doi.org/10.1021/j100266a008
25. Ben-Amotz D, Drake JM (1988) The solute size effect in rotational diffusion experiments: a test of microscopic friction theories. J Chem Phys 89:1019–1029. https://doi.org/10.1063/1.455253
26. Simon JD, Thompson PA (1990) Spectroscopy and rotational dynamics of oxazine 725 in alcohols: a test of dielectric friction theories. J Chem Phys 92:2891–2896. https://doi.org/10.1063/1.457936
27. Alavi DS, Hartman RS, Waldeck DH (1991) A test of continuum models for dielectric friction. Rotational diffusion of phenoxazine dyes in dimethylsulfoxide. J Chem Phys 94:4509–4520. https://doi.org/10.1063/1.460606
28. Goudar R, Gupta R, Kulkarni GU, Inamdar SR (2015) Rotational diffusion of a new large non polar dye molecule in alkanes. J

Fluoresc 25:1671–1679. https://doi.org/10.1007/s10895-015-1654-6
29. Horng ML, Gardecki JA, Maroncelli M (1997) Rotational dynamics of coumarin 153: time-dependent friction, dielectric friction, and other nonhydrodynamic effects. J Phys Chem A 101:1030–1047. https://doi.org/10.1021/jp962921v
30. Maroncelli M (1997) Continuum estimates of rotational dielectric friction and polar solvation. J Chem Phys 106:1545–1555. https://doi.org/10.1063/1.473276
31. Dutt GB, Raman S (2001) Rotational dynamics of coumarins: an experimental test of dielectric friction theories. J Chem Phys 114:6702–6713. https://doi.org/10.1063/1.1357797
32. Mannekutla JR, Inamdar SR, Mulimani BG, Savadatti MI (2010) Rotational diffusion of Coumarins: a dielectric friction study. J Fluoresc 20:797–808. https://doi.org/10.1007/s10895-010-0606-4
33. Inamdar SR, Mannekutla JR, Mulimani BG, Savadatti MI (2006) Rotational dynamics of nonpolar laser dyes. Chem Phys Lett 429:141–146. https://doi.org/10.1016/j.cplett.2006.08.020
34. Hughes RM, Mutzenhardt P, Bartolotti L, Rodriguez AA (2008) Experimental and theoretical analysis of the reorientational dynamics of fullerene C70 in various aromatic solvents. J Phys Chem A 112:4186–4193. https://doi.org/10.1021/jp800027j
35. Gayathri BR, Mannekutla JR, Inamdar SR (2008) Rotational diffusion of coumarins in alcohols: a dielectric friction study. J Fluoresc 18:943–952
36. Dutt GB, Rama Krishna G (2001) Rotational dynamics of coumarins in nonassociative solvents: point dipole versus extended charge distribution models of dielectric friction. J Chem Phys 115:4732–4740
37. Lackowicz JR (1983) Principles of fluorescence spectroscopy. Plenum, New York
38. Schmidt MW, Baldridge KK, Boatz JA, Elbert ST, Gordon MS, Jensen JH, Koseki S, Matsunaga N, Nguyen KA, Su S, Windus TL, Dupuis M, Montgomery JA (1993) General atomic and molecular electronic structure system. J Comput Chem 14:1347–1363
39. Renuka CG, Shivashankar K, Boregowda P, Bellad SS, Muregendrappa MV, Nadaf YF (2017) An experimental and computational study of 2-(3-Oxo3H-benzo[f] chromen-1-ylmethoxy)-benzoic acid methyl Ester. J Solut Chem 46:1535–1555. https://doi.org/10.1007/s10953-017-0661-4
40. Renuka CG, Nadaf YF, Sriprakash G, Rajendra Prasad S (2018) Solvent dependence on structure and electronic properties of 7-(Diethylamino) – 2H -1- Benzopyran −2- one (C-466) laser dye. J Fluoresc 28:839–854. https://doi.org/10.1007/s10895-018-2249-9
41. Edward JT (1970) Molecular volumes and the stokes-Einstein equation. J Chem Educ 47:261–270. https://doi.org/10.1021/ed047p2613/1.1680910
42. Fleming GR (1986) Chemical applications of ultrafast spectroscopy. Oxford University Press, London
43. Small EW, Isenberg I (1977) Hydrodynamic properties of a rigid macromolecule: rotational and linear diffusion and fluorescence anisotropy. Biopolymers 16:1907–1928
44. Sension RJ, Hochstrasser RM (1993) Comment on: rotational friction coefficients for ellipsoids and chemical molecules with slip boundary conditions. J Chem Phys 98:2490
45. Gierer VA, Wirtz K (1953) Molecular theory of microreiberation. Z. Naturforschg 8A:532-
46. Bagchi B, Jana B (2010) Solvation dynamics in dipolar liquids. Chem Soc Rev 39:1936–1954. https://doi.org/10.1039/b902048a
47. Das SK, Majhi D, Sahu PK, Sarkar M (2015) Investigation of the influence of alkyl side chain length on the fluorescence response of C153 in a series of room temperature ionic liquids. RSC Adv 5:41585–41594. https://doi.org/10.1039/C4RA16864J
48. Rosenthal SJ, Jimenez et al (1994). Solvation dynamics in methanol: Experimental and molecular dynamics simulation studies. J Mol Liq 60:25–56. https://doi.org/10.1016/0167-7322(94)00738-1
49. Simon JD (1988) Time-resolved studies of solvation in polar media. Acc Chem Res 21:128–134. https://doi.org/10.1021/ar00147a006
50. Yevheniia S, François-Alexandre M et al (2017) Solvation dynamics and rotation of coumarin 153 in a new ionic liquid/molecular solvent mixture model: [BMIM][TFSI]/propylenecarbonate. J Mol Liq 226:48–55. https://doi.org/10.1016/j.molliq.2016.10.00
51. Zhang XX, Liang M, Ernsting NP, Maroncelli M (2013) Complete solvation response of coumarin 153 in ionic liquids. J Phys Chem B 117:4291–4304. https://doi.org/10.1021/jp305430a
52. Dutta GB, Rama Krishna G (2001) Rotational dynamics of coumarins in nonassociative solvents: point dipole versus extended charge distribution models of dielectric friction. J Chem Phys 115:4732–4741. https://doi.org/10.1063/1.1395563
53. Dutt GB (2000) Rotational dynamics of non-dipolar probes in alkane–alkanol mixtures: microscopic friction on hydrogen bonding and non-hydrogen bonding solute molecules. J Chem Phys 113:11154–11158
54. Alavi DS, Waldeck DH (1991) Rotational dielectric friction on a generalized charge distribution. J Chem Phys 94:6197–6202
55. Hartman RS, Waldeck DH (1994) Rotational diffusion of fluorenes in Dimethyl Sulfoxide. J Phys Chem 98:1386–1393
56. Hartman RS, Waldeck DH (1991) An experimental test of dielectric friction models using the diffusion of aminoanthraquinones. J Phys Chem 95:7872–7880
57. Kurnikova MG, Waldeck DH, Coalson RD (1996) A molecular dynamic study of dielectric friction. J Chem Phys 105:628–638
58. Panwang Z, Jianyon L, Peng S, Heli K, Guozhing H (2009) Rotational reorientation dynamics of rhodamine 700 in different excited states. J Lumin 129:283–289